Scale-Dependent Photosalience and Topotactic Reaction of Microcrystalline Benzylidenebutyrolactone Determined by Electron Microscopy and Electron Diffraction

Vince M. Hipwell,[a] Chih-Te Zee,[a] Jose Rodriguez*,[a] and Miguel A. Garcia-Garibay*[a]

[a]Department of Chemistry and Biochemistry, University of California, Los Angeles, California 90024-1569.

*Email: jrodriguez@mbi.ucla.edu, mgg@chem.ucla.edu

ABSTRACT: The macroscopic motion of crystals induced by a solid-state photochemical reaction, also known as photosalience, is of interest for the development of micromechanical actuators and crystalline molecular machines. Using microcrystal electron diffraction, we report evidence for a minimum crystal size threshold below which photosalience is not observed for benzylidenebutyrolactone. We confirm our observations by solving the crystal structure of micron-scale specimens before and after their topotactic single crystal-to-single crystal reaction, and by collecting transmission electron microscopy images that reveal the absence of photosalient effects for crystals that are below *ca*. 10 μm in size. These results indicate that photosalience depends not only on the ability of crystals to support a photochemical reaction, but also on a size threshold where the accumulated product phase can form a layer that is separate from that of the reactant, such that their different packing dimensions are able to transduce the collective strain accumulated at the molecular level boundaries into the macroscopic motion that propels the entire crystal specimen.

Photosalience is an interesting, emergent phenomenon that involves the macroscopic motion of crystals.[1] It occurs as a result of photochemical reactions in their crystalline phase,[2,3] although recent results suggest that photothermal effects can also play a small role under some circumstances.[4] Photosalience is thought to be the result of the collective or sudden release of strain that is built up between the grain boundaries of segregated reactant and product crystalline domains, along with more complex and subtle processes.[1–7] As shown in Scheme 1, photosalience can be illustrated in a simple manner by considering a single crystal exposed to light that causes a chemical reaction up to certain sample depth. Photosalience occurs when changes in volume between the reactant and product are manifested in the form of a relative expansion or contraction that leads to generation of mechanical stress that is eventually released in the form of macroscopic motion. In this paper, we investigate the well-established photosalience of crystalline benzylidenebutyrolactone **1** (Scheme 1) in order to determine whether this phenomenon has a size threshold in the nanometer or submicron scale through a combination of micro-electron diffraction (microED) and TEM imaging.[8] Our results indicate that crystals of all sizes facilitate the SCSC photodimerization reaction shown in Scheme 1, but only crystals beyond certain size are able to exhibit photosalience. We conclude that photochemical reactions in nanocrystals with sizes of the same order of magnitude as wavelength of light occur in a relatively homogeneous manner,[9] and we discuss the size limit at which photosalience occurs as well as a hypothesis for the change in behavior.

Photosalience in crystals of **1** has been studied in great detail by Naumov and coworkers using optical microscopy and high-speed cameras to catalogue different types of motion and their relation to the size and aspect ratios of the crystals.[10] The crystals analyzed by this method had sizes of 20–240 μm along their shortest dimension and 0.19–2.8 mm along the longest one. While it may be possible to investigate even smaller crystals with optical microscopy, the lower limit is fundamentally restricted by the maximum magnification achievable with this method. Thus, in order to establish the existence or lack of

Scheme 1

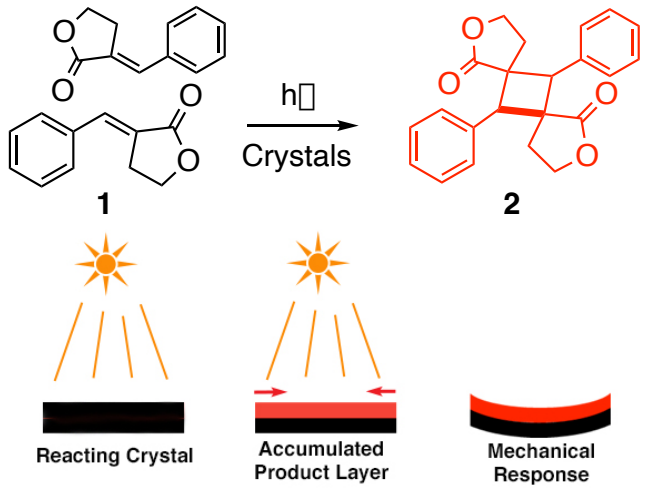

photosalience in nanocrystals and small microcrystals of **1**, we turned to the use of electron microscopy.

Compound **1** was synthesized as reported in the literature and photochemical experiments carried out with polycrystalline samples showed that it undergoes the expected quantitative dimerization reaction to the trans- head-to-tail cyclobutane **2** (Scheme 1 and Figures S3-S4). Powder X-ray diffraction (PXRD) patterns obtained before and after irradiation and comparison with those simulated from single crystal structure data of **1** and **2** confirmed the identity of the crystal phases as those of the previously analyzed crystal forms (Figure S5).[10]

Samples for microED experiments were prepared as aqueous suspensions using the reprecipitation method.[11] A stock solution of 30 mg/mL (40 μL) of **1** in acetonitrile was added to 4.0 mL of rapidly vortexing Millipore water by micropipette. Multiple droplets of these suspensions were drop-cast onto a TEM grid, then wicked away with filter paper held parallel to the surface of the grid on the outer edge of the suspension droplet. TEM imaging of grids prepared by this method revealed relatively sparse loading of crystalline material. Despite this, a

sufficient number of crystals were found to enable structure solution.

Diffraction data was collected on a Tecnai TF30 microscope from multiple microcrystals before and after UV-irradiation using a 450 W Hanovia medium-pressure mercury lamp. Following data collection on the crystals of **1**, the sample holder was removed and transferred to the photochemical reactor without removing the grid. The crystals were irradiated for 10 minutes in the Hanovia reactor. The sample holder was then replaced in the TEM system and post-irradiation diffraction data was collected from the same crystals based on positions saved on the TEM computer system.

Crystal structures of **1** and **2** were determined from the same set of 5 crystals before and after UV irradiation, as shown in Figure 1 along with images of a subset of these crystals. Approximate sizes can be estimated for these crystals in relation to the red dotted circles, which denote the size and position of the ~5 μm selected area aperture. Notably, these images show that each crystal remained in the same position and orientation before and after irradiation, suggesting that the photosalient effects previously observed using an optical microscope with larger crystals of this compound were not active in crystals of this size.

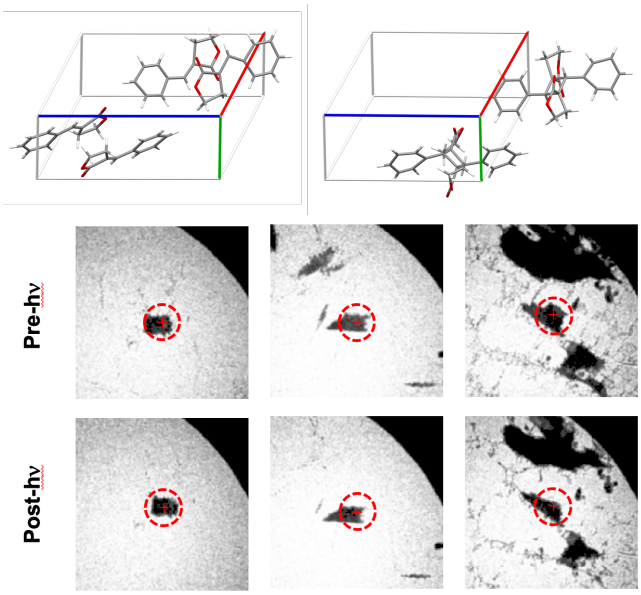

Figure 1. (Top) Crystal structures of **1** and **2** determined by microED from a set of 5 crystals before and after UV irradiation. (Bottom) TEM images of 3 of these crystals. The red dotted circles indicate the position and size of the ~5 micron selected area aperture.

Notably, NMR analysis of similar aqueous suspensions of **1** before and after UV irradiation revealed that the topotactic reaction to form **2** constituted a very small portion (< 1 %) of the observed photochemical reactivity. The dominant reaction pathway in this case was the (E) to (Z) isomerization to **1**, as determined by ^{1}H NMR analysis following extraction of the irradiated suspension with DCM (Figure S6). This observation suggested significant water solubility for compound **1**, which was demonstrated by ^{1}H NMR using an internal standard. We discovered that suspensions prepared in this manner contain up to 47 % of **1** in equilibrium in solution (Figure S7). While this observation does not affect the topotactic reaction and electron diffraction analysis shown in Figure 1, it has important implications on the observed lack of photosalience, as it may be possible that crystals deposited from aqueous suspension adhered to the surface of the TEM grid by solubilized and subsequently dried material that may act as glue.[12] To test this possibility, we prepared additional samples by direct loading of polycrystalline powders. TEM grids were gently dropped and submerged in the powder of **1** in a sample vial, then removed with tweezers. Excess powder was removed by tapping the tweezers on the edge of the vial.

Following the same diffraction data collection procedure described above, crystal structures were solved before and after irradiation of a single crystal (Figure 2). We speculate that the necessity to combine data from multiple crystal specimens in the case of the suspension samples may be due to the water-solubility of **1**, which may lead to a higher percentage of crystal defects, twinning, or potential deposit of amorphous phases.

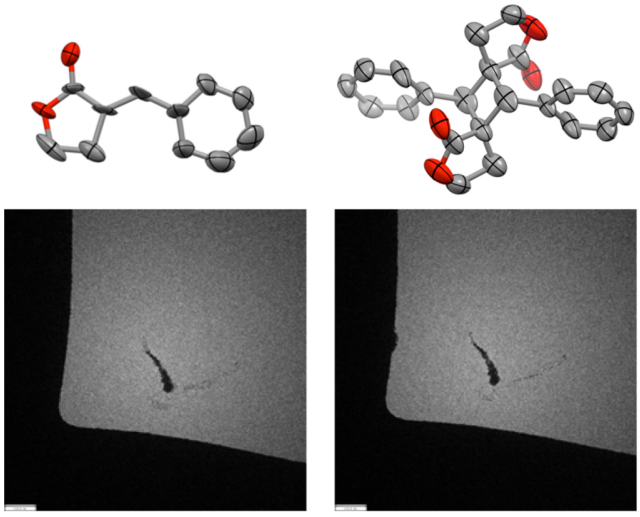

Figure 2. (Top) Single crystal electron diffraction structures of **1** and **2**. (Bottom) Low resolution images of the single microcrystal before and after irradiation obtained in diffraction mode.

For the next set of experiments we collected images of microcrystals from the powder sample before and after irradiation. TEM grids were loaded in the same manner as described above, then screened in diffraction mode to find suitable crystals. For smaller crystals, a single diffraction pattern at 0° tilt angle was collected to verify crystallinity. This was not possible for larger crystals that were too thick to enable adequate penetration of the electron beam, but the images display clearly faceted specimens. Furthermore, knowing from the bulk solid irradiation that > 99 % of the powder sample is indeed crystalline, we assumed that any material deposited and imaged on the TEM grid was also crystalline. High-resolution real-space images were obtained for crystals ranging in size from ca. 400 nm to > 100 μm. After the standard UV irradiation procedure, a second set of images was taken at the same locations on the TEM grid. Repre-

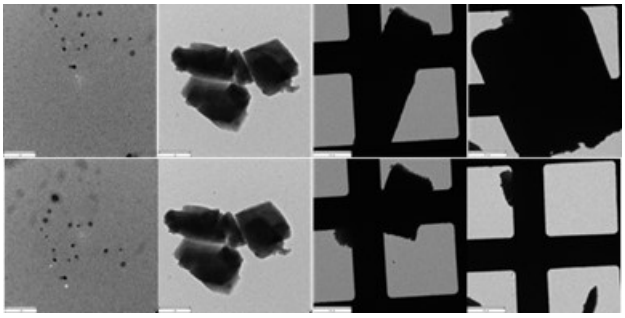

Figure 3. Representative images of nanocrystals and microcrystals before (top) and after (bottom) irradiation. The scale bar for the first two images from the left is 1 μm and that for the last two images is 30 μm.

sentative pre- and post-irradiation images of each crystal or set of crystals are shown in Figure 3. The complete set of images can be found in Figures S8 and S9. The results shown in Figure 3 confirm that there is a size-dependent threshold for the observation of the photosalient effect. All the nanocrystals and the small microcrystals were found to be in the exact same position and orientation after irradiation, whereas a majority of crystals ~100 μm or longer along their largest dimension had either fractured or moved out of the frame entirely.

To verify that the motion of the larger crystals was not induced by the handling and movement of the grid holder, a control experiment was conducted in which images were taken before and after handling the grid holder in the same manner, but without irradiation. These images can be found in the SI, and they show that crystals in the same size range remain in the same positions.

With this relatively limited set of crystal specimens, an exact description of the shape and size of crystals of **1** at which photosalience begins to occur cannot yet be established. Notably, it has been shown that crystals of other compounds which are submicron in at least one dimension, such as crystalline nanorods, still exhibit a bending motion.[13–16] Consideration of the aspect ratios of the crystals at these smaller length scales may also be a factor which controls photosalience. Therefore, it should be noted that there may be a dependence based on the third dimension normal to the plane of the TEM grid, which cannot be quantified from these images. Nonetheless, these results demonstrate a striking difference of behavior of crystals in different size regimes. It can be said that crystals of **1** with dimensions that range from nanocrystalline, or sub-micron in all dimensions, up to ~50 μm in the largest dimension may not exhibit photosalience. As shown in Figure 4, SEM imaging of a powder sample of **1** reveals the approximate depth of crystals that are similar in size to those which exhibited photosalience. It is interesting to note that this depth seems to be similar to that which would lead to almost complete absorption of incident photons. Taking the extinction coefficient of **1** and calculating its concentration in crystals one can estimate that a speciments with a ca. 10 μm in depth would have a 1 % transmittance at the λ_{max} of 282 nm, under the assumption that dependence on molecular orientation within the crystal (which leads to a bias in the average orientation of the transition dipole moment) has minimal impact. The UV-vis spectrum of **1** along with the calibration curve to determine the extinction coefficient can be found in the SI. The absorption spectrum and this calculation was also utilized to produce the plot in Figure 4, which shows crystal depth corresponding to 1 % transmittance as a function of wavelength.

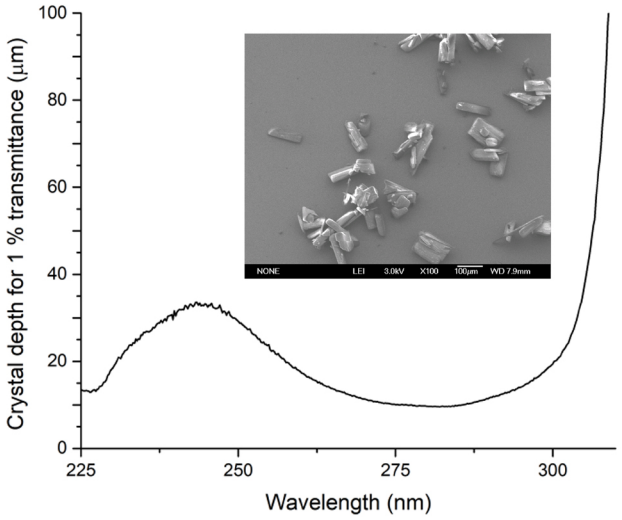

Figure 4. Light penetration depth corresponding to 1 % transmittance as a function of wavelength for crystals of **1.** The inset is a SEM image from a polycrystalline powder viewed with 20° tilt to show approximate crystal depth .

This size-dependent threshold demonstrates that photosalience is an emergent phenomenon that relies not only on a particular arrangement of a photochemically-active compound within a crystal, but also on the mechanical and photochemical properties of the crystal itself. The smaller crystals may be more elastic, and therefore better able to accommodate any strain that is formed between reactant and product crystal grain boundaries. Diffraction associated with lattice deformation or ripples on the nanoscale has recently been associated with rigid peptide nanocrystals (Gallagher-Jones *et al*. 2019). Furthermore, the higher surface-area-to-volume ratio of the smaller crystals would promote more homogeneous irradiation throughout the crystal, which would mitigate the segregation of different crystal domains.[17]

In conclusion, we have demonstrated the use of microED to determine crystal structures from a single microcrystal before and after an SCSC reaction. In addition, a TEM imaging study established that photosalience is an emergent multiscale phenomenon with a size threshold. Given the renewed interest in mechanically-responsive crystals for use as nano- and micromechanical actuators,[18–22] this size-dependent behavior may place a lower limit on the size of mechanical devices that can be constructed with such crystals as actuating components. This is particularly true if this size dependence is a general effect observed in all mechanically-responsive crystals.

ASSOCIATED CONTENT

Supporting Information.

Sample preparation and characterization including powder X-ray diffraction, TEM images, crystallographic data (pdf) as well as CIF files.

AUTHOR INFORMATION

Corresponding Author

* Miguel A. Garcia-Garibay, mgg@chem.ucla.edu
* Jose Rodriguez, jrodriguez@mbi.ucla.edu

Funding Sources

This work was supported by NSF grant CHE-1855342

ACKNOWLEDGMENT

Support from the UCLA Graduate Division for V.M.H. and C.Z. with dissertation year fellowships is gratefully acknowledged.

REFERENCES

(1) Naumov, P.; Chizhik, S.; Panda, M. K.; Nath, N. K.; Boldyreva, E. Mechanically Responsive Molecular Crystals. *Chem. Rev.* **2015**, *115*, 12440–12490.

(2) Rath, B.B.; Vittal, J.J. Single-Crystal-to-Single-Crystal [2+2] Photocycloaddition Reaction in a Photosalient One-Dimensional Coordination Polymer of Pb(II). *J. Am. Chem. Soc.* **2020**, *142*, 20117-20123

(3) Zhu, L.; Al-Kaysi, R. O.; Bardeen, C. J. Photoinduced Ratchet-Like Rotational Motion of Branched Molecular Crystals. *Angew. Chemie - Int. Ed.* **2016**, *55*, 7073–7076.

(4) Hasebe, S.; Hagiwara, Y.; Komiya, J.; Ryu, M.; Fujisawa, H.; Morikawa, J.; Katayama, T.; Yamanaka, D.; Furube, A.; Sato, H.; Asahi, T.; Koshima, H. Photothermally Driven High-Speed Crystal Actuation and Its Simulation. *J. Am. Chem. Soc.* **2021**, *143*, 8866–8877.

(5) Desta, I. T.; Chizhik, S. A.; Sidelnikov, A. A.; Karothu, D. P.; Boldyreva, E. V.; Naumov, P. Mechanically Responsive Crystals: Analysis of Macroscopic Strain Reveals "Hidden" Processes. *J. Phys. Chem. A* **2020**, *124*, 300–310.

(6) Kearsley, S. K.; Desiraju, G. R. Determination of an Organic Crystal Structure with the Aid of Topochemical and Related Considerations: Correlation of the Molecular and Crystal Structures of α-Benzylidene-γ-Butyrolactone and 2- Benzylidenecyclopentanone With Their Solid State Photoreactivity. *Proc. R. Soc. Lond. A* **1985**, *397*, 157–181.

(7) Jones, C. G.; Martynowycz, M. W.; Hattne, J.; Fulton, T. J.; Stoltz, B. M.; Rodriguez, J. A.; Nelson, H. M.; Gonen, T. The CryoEM Method MicroED as a Powerful Tool for Small Molecule Structure Determination. *ACS Cent. Sci.* **2018**, *4*, 1587–1592.

(8) Rodriguez, J. A.; Eisenberg, D. S.; Gonen, T. Taking the Measure of MicroED. *Curr. Opin. Struct. Biol.* **2017**, *46*, 79–86.

(9) Chin, K. K.; Natarajan, A.; Gard, M.; Campos, L. M.; Johansen, E.; Shepherd, H.; Garcia-Garibay, M. A. Organic Molecular Nanocrystals: Triplet–Triplet Absorption, Phosphorescence, and Circular Dichroism of Chiral Crystals of Benzophenone. *Chem. Comm* **2007**, 4266-4268.

(10) Nath, N. K.; Runčevski, T.; Lai, C. Y.; Chiesa, M.; Dinnebier, R. E.; Naumov, P. Surface and Bulk Effects in Photochemical Reactions and Photomechanical Effects in Dynamic Molecular Crystals. *J. Am. Chem. Soc.* **2015**, *137*, 13866–13875.

(11) Kasai, H.; Nalwa, H. S.; Oikawa, H.; Okada, S.; Matsuda, H.; Minami, N.; Kakuta, A.; Ono, K.; Mukoh, A.; Nakanishi, H. A Novel Preparation Method of Organic Microcrystals. *Jpn. J. Appl. Phys.* **1992**, *31*, L1132–L1134.

(12) Blelloch, N. D.; Mitchell, H. T.; Tymm, C. C.; Van Citters, D. W.; Mirica, K. A. Crystal Engineering of Molecular Solids as Temporary Adhesives. *Chem. Mater.* **2020**, *32,* 9882–9896

(13) Al-Kaysi, R. O.; Bardeen, C. J. General Method for the Synthesis of Crystalline Organic Nanorods Using Porous Alumina Templates. *Chem. Commun.* **2006**, *No. 11*, 1224–1226.

(14) Al-Kaysi, R. O.; Bardeen, C. J. Reversible Photoinduced Shape Changes of Crystalline Organic Nanorods. *Adv. Mater.* **2007**, *19*, 1276–1280.

(15) Good, J. T.; Burdett, J. J.; Bardeen, C. J. Using Two-Photon Excitation to Control Bending Motions in Molecular-Crystal Nanorods. *Small* **2009**, *5*, 2902–2909.

(16) Kim, T.; Al-Muhanna, M. K.; Al-Suwaidan, S. D.; Al-Kaysi, R. O.; Bardeen, C. J. Photoinduced Curling of Organic Molecular Crystal Nanowires. *Angew. Chemie - Int. Ed.* **2013**, *52*, 6889–6893.

(17) Al-Kaysi, R. O.; Müller, A. M.; Bardeen, C. J. Photochemically Driven Shape Changes of Crystalline Organic Nanorods. *J. Am. Chem. Soc.* **2006**, *128*, 15938–15939.

(18) Manrique-Juárez, M. D.; Rat, S.; Salmon, L.; Molnár, G.; Quintero, C. M.; Nicu, L.; Shepherd, H. J.; Bousseksou, A. Switchable Molecule-Based Materials for Micro- and Nanoscale Actuating Applications: Achievements and Prospects. *Coord. Chem. Rev.* **2016**, *308*, 395–408.

(19) Kim, T.; Zhu, L.; Al-Kaysi, R. O.; Bardeen, C. J. Organic Photomechanical Materials. *ChemPhysChem.* **2014**, *15*, 400–414.

(20) Nath, N. K.; Panda, M. K.; Sahoo, S. C.; Naumov, P. Thermally Induced and Photoinduced Mechanical Effects in Molecular Single Crystals - A Revival. *CrystEngComm* **2014**, *16*, 1850–1858.

(21) Commins, P.; Desta, I. T.; Karothu, D. P.; Panda, M. K.; Naumov, P. Crystals on the Move: Mechanical Effects in Dynamic Solids. *Chem. Commun.* **2016**, *52*, 13941–13954.

(22) Sato, O. Dynamic Molecular Crystals with Switchable Physical Properties. *Nat. Chem.* **2016**, *8*, 644–656.

"For Table of Contents Use Only,"

Scale-Dependent Photosalience and Topotactic Reaction of Microcrystalline Benzylidenebutyrolactone Determined by Electron Microscopy and Electron Diffraction

Vince M. Hipwell, Chih-Te Zee, Jose Rodriguez, and Miguel A. Garcia-Garibay

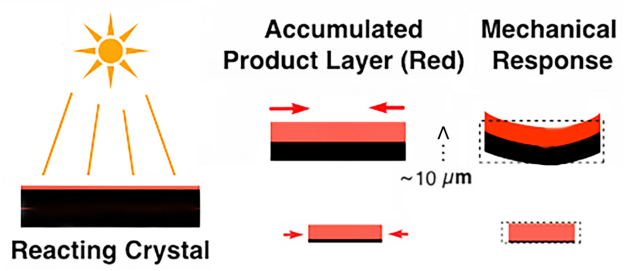

Synopsis: Taking advantage of micro-electron diffraction (micro-ED) and imaging, it was possible to confirm the lower limit of the size-dependence of the phenomenon known as photosalience, where single crystals of benzylidenebutyrolactone undergoing a topotactic photodimerization were seen to jump, roll, bend or break upon light excitation only when their sizes were above ca. 10 μm.